International Journal of Nanomedicine

Dovepress
open access to scientific and medical research

Open Access Full Text Article

ORIGINAL RESEARCH

Ultrasmall superparamagnetic Fe_3O_4 nanoparticles: honey-based green and facile synthesis and in vitro viability assay

This article was published in the following Dove Press journal:
International Journal of Nanomedicine

Elisa Rasouli[1]
Wan Jeffrey Basirun[2]
Majid Rezayi[3,4]
Kamyar Shameli[5]
Esmail Nourmohammadi[6]
Roshanak Khandanlou[7]
Zahra Izadiyan[5]
Hoda Khoshdel Sarkarizi[8]

[1]Nanotechnology & Catalysis Research Centre, Institute of Postgraduate Studies, University of Malaya, Kuala Lumpur, Malaysia; [2]Department of Chemistry, Faculty of Science, University of Malaya, Kuala Lumpur, Malaysia; [3]Medical Toxicology Research Center, Mashhad University of Medical Sciences, Mashhad, Iran; [4]Department of Modern Sciences and Technologies, School of Medicine, Mashhad University of Medical Sciences, Mashhad, Iran; [5]Malaysia-Japan International Institute of Technology, University Technology Malaysia, Kuala Lumpur, Malaysia; [6]Department of Medical Biotechnology, School of Medicine, Mashhad University of Medical Sciences, Mashhad, Iran; [7]School of Psychological and Clinical Sciences, Faculty of Engineering, Health, Science and the Environment, Charles Darwin University, Darwin, NT, Australia; [8]Department of Anatomical Sciences and Cell Biology, School of Medicine, Mashhad University of Medical Sciences, Mashhad, Iran

Correspondence: Wan Jeffrey Basirun
Department of Chemistry, Faculty of Science, University of Malaya, Wilayah Persekutuan Kuala Lumpur, Kuala Lumpur 50603, Malaysia
Tel +60 12 935 4200
Email jeff@um.edu.my

Introduction: In the present research, we report a quick and green synthesis of magnetite nanoparticles (Fe_3O_4-NPs) in aqueous solution using ferric and ferrous chloride, with different percentages of natural honey (0.5%, 1.0%, 3.0% and 5.0% w/v) as the precursors, stabilizer, reducing and capping agent, respectively. The effect of the stabilizer on the magnetic properties and size of Fe_3O_4-NPs was also studied.

Methods: The nanoparticles were characterized by X-ray diffraction (XRD) analysis, field emission scanning electron microscopy, energy dispersive X-ray fluorescence, transmission electron microscopy (TEM), vibrating sample magnetometry (VSM) and Fourier transform infrared spectroscopy.

Results: The XRD analysis indicated the presence of pure Fe_3O_4-NPs while the TEM images indicated that the Fe_3O_4-NPs are spherical with a diameter range between 3.21 and 2.22 nm. The VSM study demonstrated that the magnetic properties were enhanced with the decrease in the percentage of honey. In vitro viability evaluation of Fe_3O_4-NPs performed by using the MTT assay on the WEHI164 cells demonstrated no significant toxicity in higher concentration up to 140.0 ppm, which allows them to be used in some biological applications such as drug delivery.

Conclusion: The presented synthesis method can be used for the controlled synthesis of Fe_3O_4-NPs, which could be found to be important in applications in biotechnology, biosensor and biomedicine, magnetic resonance imaging and catalysis.

Keywords: honey, Fe_3O_4 nanoparticles, green synthesis, transmission electron microscopy, magnetic properties, in vitro, viability, MTT assay, WEHI164 cells

Introduction

Recently, rapid advancement in nanotechnology has made synthesis, characterization and improvement of nanoparticles in terms of functional properties possible for various applications. The inspiration for the synthesis of artificial materials for the better quality and quantity comes from nature. The extensive application of metal nanoparticles in different fields, especially in biotechnology, has motivated the metal nanoparticles synthesis.[1] Nanoparticles has attracted incredible attention because of their smaller size and larger surface area compared with bulk materials, in addition to having novel biological and mechanical properties, optical absorption, electrical conductivity and catalytic activity.[2–4]

Among the different types of nanoparticles, magnetic nanoparticles, especially magnetite and maghemite nanoparticles with proven biological properties and good biocompatibility, have been the subject of various studies, due to the wide range of important biomedical and environmental applications such as cancer hyperthermia therapy, drug delivery, cell labeling, enhanced magnetic resonance imaging and magnetic

submit your manuscript | www.dovepress.com
Dovepress
http://dx.doi.org/10.2147/IJN.S158083

separation. So far, the synthesis and preparation of iron oxide nanoparticle has been an important research priority, and it has been extensively studied and characterized.[5–7]

Over the past decade, numerous methods have been proposed for the synthesis of magnetite nanoparticles (Fe_3O_4-NPs), including physical, chemical and biological methods. These include methods such as microemulsions, coprecipitation of ferrous and ferric ions aqueous solution using a base,[8–10] sol–gel method,[11] sonochemistry,[12] colloidal method,[13] nonaqueous route,[14] pyrolysis reaction,[15] thermal decomposition of organic iron precursor in organic solvents,[16–18] solvothermal synthesis,[19] hydrothermal synthesis,[20,21] mechano-chemical processing[22] and emulsion techniques.[23,24] Although, bulk chemical synthesis of large amount of nanoparticles is fast and simple, to obtain the effective size stabilization of the nanoparticles, it is important to use capping agents. Furthermore, some of the chemicals used in the synthesis and stabilization are harmful and could produce noneco-friendly, unsafe and hazardous products, and therefore there is a growing demand for the use of green technology in the synthesis of nanoparticles. Thus, new and advanced methods for the growth of nanoparticles must draw inspiration from biological systems.[25–27]

Honey is one of the most beneficial foods accessible, which largely consists of fructose and glucose. Also, it is rich in amino acids, essential minerals, vitamin C and enzymes. Honey has been subjected to broad study throughout the world.[5–9] It contains antioxidants, which are important in cancer prevention.[20] Recently, aqueous synthesis of silver nanoparticles utilizing natural honey has been reported.[21]

In this work, Fe_3O_4-NPs are synthesized using iron (III) chloride, iron (II) chloride, sodium hydroxide and natural honey at room temperature through a fast precipitation method. The reaction was completed under optimal conditions, and low cost and energy using friendly environment and fresh, nontoxic materials, solvents and also inert residue materials. The synthesis method is based on green chemistry, which is a main step toward safer synthesis and preparation of nanoparticles. To the best of our knowledge, there is no report on the synthesis and characterization of Fe_3O_4-NPs using natural honey as a stabilizer and co-reducing agent.

Materials and methods

Materials and reagents

All chemicals used in this study were utilized without further purification and were of analytical grade. Chemicals used for the synthesis of Fe_3O_4-NPs, such as $FeCl_3{\cdot}6H_2O$ and $FeCl_2{\cdot}4H_2O$ (99.89%), were obtained from Merck (Frankfurt, Germany), natural honey was collected from the unpolluted cold highlands of Northeastern China, and NaOH (99.0%) was provided by Merck (Frankfurt, Germany). Deionized water was used to prepare all solutions. Glassware was cleaned in HNO_3/HCl (3:1, v/v) solution, washed with deionized water and dried before use.

Preparation of Fe_3O_4 nanoparticles

In the synthesis of Fe_3O_4-NPs, different amounts of natural honey 0.5, 1.0, 3.0 and 5.0 g were added to 100 mL of deionized water, as the coprecipitation agent and stabilizer to control the particle size. Then $FeCl_3{\cdot}6H_2O$ and $FeCl_2{\cdot}4H_2O$ (with a 2:1 molar ratio) were added under continuous stirring and nitrogen gas bubbling to inhibit oxidation. The mixture was titrated against a NaOH (2.0 M) solution under continuous stirring until the pH reached 10. The Fe_3O_4-NPs were formed instantly from the reduction procedure. The resulting black suspension was centrifuged, washed three times with the deionized water and ethanol mixure and then dried in an oven at 60°C.

Characterization methods and instruments

The phase structure of the nanoparticles was obtained by X-ray diffraction (Cu Kα 1.5406 Å radiation), using a Bruker D8 Advance diffractometer (Bruker AXS, Billerica, MA, USA) at room temperature between 20°–25°, in the 2q scale, with a scanning speed of 0.02°/s and a step time of 3 seconds. Transmission electron microscopy (TEM) was done using a Tecnai G2 F20 transmission electron microscope from FEI (USA), with an acceleration voltage of 200 kV. The size distributions of particles were identified using the ImageJ version 1.46 r program. The morphology of the Fe_3O_4-NPs was determined through Field emission scanning electron microscopy (FESEM). FESEM and energy-dispersive X-ray (EDX) spectroscopy were performed using Quanta™ 450 FEG, Oxford instrument (USA). The dried samples were coated with gold using a sputter coater. A vibrating sample magnetometer (VSM) was used to study the magnetic properties of the samples utilizing a VSM, Lake Shore Model 7400, Tokyo, Japan, with magnetic fields up to 8 kOe. Fourier transform infrared spectroscopy (FT-IR) was performed between 400 and 4,000 cm^{-1} to characterize possible biomolecules that are responsible for the capping and efficient stabilization of the Fe_3O_4-NPs. The FT-IR spectra were observed using a Spectrum 400 FT-IR/FT-FIR spectrometer (Perkin Elmer, Waltham, MA, USA).

Results and discussion

As shown in Figure 1, once NaOH solution was added as a reducing agent to the honey aqueous mixture with Fe^{3+} and Fe^{2+} chloride (2:1 molar ratio), the color of suspension turned black and the Fe_3O_4-NPs were easily separated by a magnet.

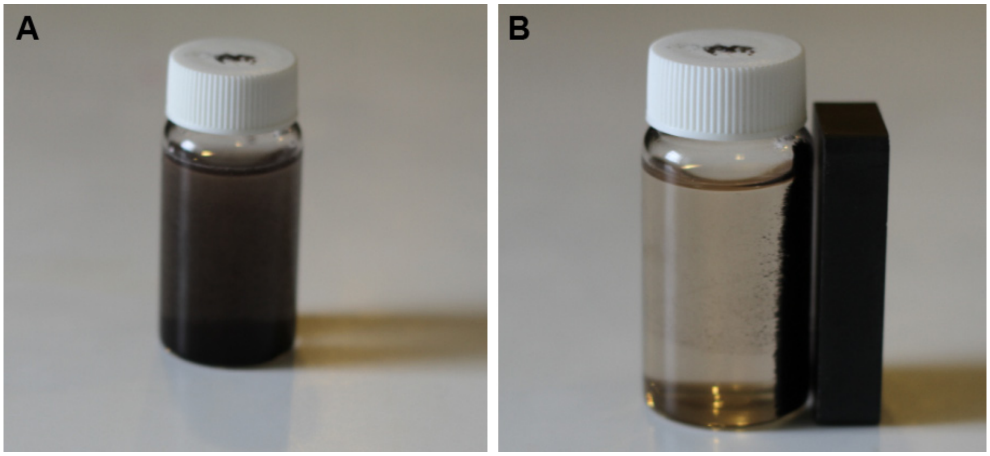

Figure 1 The 0.5% (w/v) honey/magnetite nanoparticles suspension without (**A**) and with (**B**) a magnetic field.

The chemical reaction for the precipitation of Fe_3O_4 is as follows:

$$\begin{aligned} & FeCl_2 \cdot 4H_2O + 2FeCl_3 \cdot 6H_2O + 8NaOH \\ & \rightarrow Fe_3O_4 + 8NaCl + 20H_2O \end{aligned} \tag{1}$$

Phase structure of nanoparticles

The Fe_3O_4-NPs were characterized through X-ray powder diffraction (XRD) and all the peaks were analyzed and indexed using the ICDD database, by comparing with the magnetite standards (Figure 2).[28] The peaks were indexed to the (220, 311, 400, 422, 511, 440) and (533) planes, which is attributed to the 2θ of 30.46°, 35.76°, 43.51°, 53.24°, 56.88°, 63.32° and 71.41°, respectively, with the standard diffraction spectrum (ref. code Fe_3O_4:01-088-0315).[29]

Generally, the diffraction peaks with less intensity in the XRD pattern show the small size of the Fe_3O_4-NPs. In this case, there is a decreased intensity of the peaks with increasing honey concentration, which also indicates the decrease in the particle size.

FT-IR spectra analysis

Honey contains proteins, minerals, vitamins and natural sugars (mostly fructose, sucrose and glucose).[30–34] Fourier transform infrared spectroscopy (FT-IR) was performed to

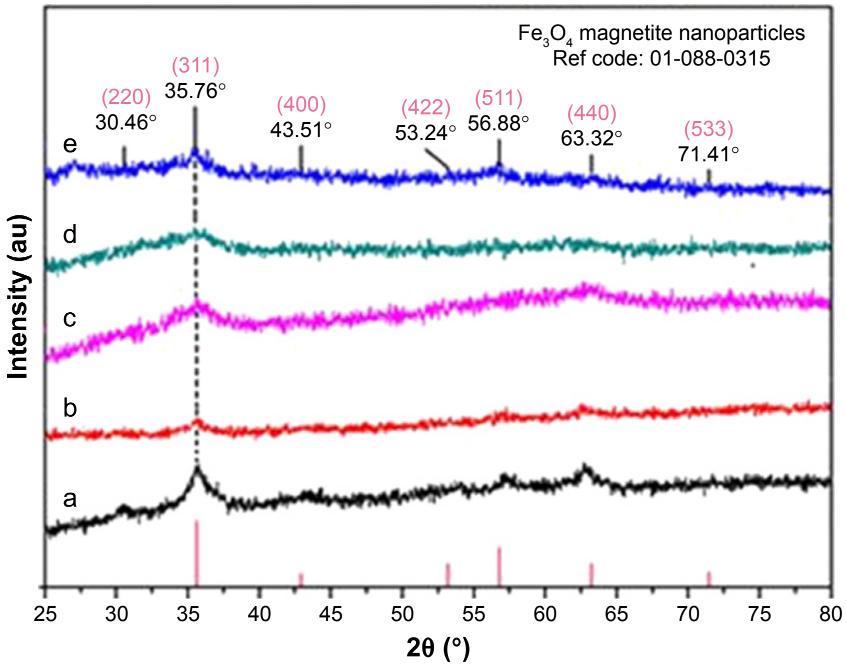

Figure 2 Powder X-ray diffraction patterns of Fe_3O_4-NPs without (**a**) and with different concentrations of honey (0.5, 1, 3, and 5% [w/v]) (**b**–**e**), respectively.
Abbreviations: Fe_3O_4-NPs, magnetite nanoparticles; ref, reference.

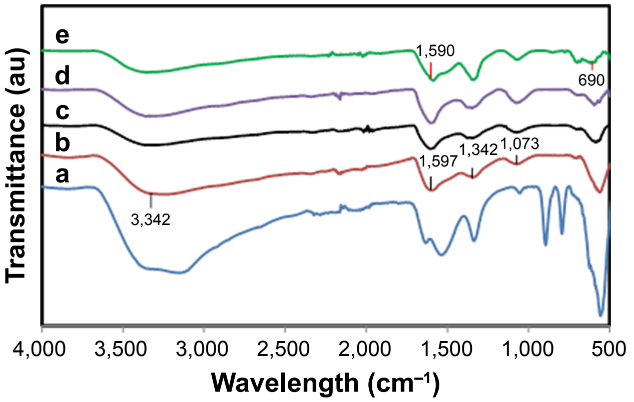

Figure 3 Fourier-transform infrared spectra of honey (**a**); magnetite nanoparticles with 0.5, 1, 3, and 5% (w/v) honey (**b**–**e**, respectively).

determine the potential biomolecules that are responsible for efficient stabilization and also capping of Fe_3O_4-NPs synthesized using honey. The FT-IR spectrum in Figure 3 shows a strong absorption band at 564.99 cm^{-1}, which is assigned to the Fe–O bond, demonstrates a high grade of crystallinity of the Fe_3O_4-NPs.[35] The absorption band at 609.45 cm^{-1} in the FT-IR spectrum of sample (Figure 3e) indicates the presence of some amount of oxidized maghemite on the surface of magnetite. The characteristic band around 3,200 cm^{-1} is due to the existence of the O–H group.[36]

The C–O stretching mode merges band of protein in honey arise from the C–O–C symmetric stretching and C–O–H bending vibrations, expected to occur around 1,073 cm^{-1}.[37] The amide I and II bands of proteins are expected to occur around 1,660 and 1,535 cm^{-1}, respectively,[38–43] in the current study, these bands occurred around 1,600 and 1,300 cm^{-1}. These bands occur as a result of the carboxyl stretching and N–H deformation vibrations in the amide linkages of protein. Proteins can attach to the Fe_3O_4-NPs via the free amine group or carboxylate ion of amino acid residues.[41,44,45] The lack of C=O band because of the stretching mode, the existence of the C–O stretch and amide I and II bands in the FT-IR spectrum (Figure 3) of Fe_3O_4-NPs represent the stabilization of the system by the –COO– (carboxylate ion) groups of amino acid remains with free carboxylate groups in the proteins.

Size distribution and morphology of nanoparticles

TEM micrographs of the particle size and distribution of the Fe_3O_4-NPs are presented in Figure 4. The images reveal significantly smaller nanomagnetite particles with identical particle sizes which have similar shape and are uniformly dispersed. Also, the Fe_3O_4-NPs have spherical morphology and a uniform distribution. From the TEM images, it is obvious that the particle size decreases from 3.21 to 2.22 nm for 0.5% and 3.0% (w/v) with the increase in the amount of honey. It is significant to mention that sucrose, glucose (decomposition product of sucrose) and gluconic acid have multiple hydroxyl groups, apart from the carboxylic groups in gluconic acid, in the magnetite synthesis. These functional groups can be absorbed into define crystal planes or chelated with the Fe atoms as a covering material to create steric block, like the common stabilizers and surfactants.[46]

The FESEM images show that the Fe_3O_4-NPs synthesized using honey have spherical structure (Figure 5). Significantly, no morphological differences were detected with the increase in the honey concentration and confirm that the structure of the nanoparticles remained unchanged. Figure 6 shows the chemical composition of the prepared nanoparticles. From the EDX spectrum, the oxygen and iron peaks reveal the existence of Fe_3O_4-NPs; the peaks that arise around 0.7, 6.4 and 7 keV are corresponding to the Fe element.[47] Besides, the EDX spectra of the Fe_3O_4-NPs confirm the presence of elemental Fe without any impurity peaks.

Magnetic properties of nanoparticles

The magnetic characterization of the Fe_3O_4-NPs was performed with VSM. Figure 7 presents the hysteresis loop of all samples measured with a magnetic field of –8,000 to 8,000 Oe at room temperature. Samples (a), (b), (c), (d) and (e) display almost immensurable coercivity and remanence, indicating that the magnetic nanoparticles prepared are superparamagnetic.[48]

The saturation magnetization (M_s) of Fe_3O_4-NPs with 5.0, 3.0, 1.0 and 0.5% (w/v) honey are 2.19, 3.75, 6.25 and 19.91 emu g^{-1}, respectively, which increases with the decrease in the honey concentration. This might be referring to the decrease of the surface adsorbed species and growth of the particle size.[49] The VSM shows that the M_s of the Fe_3O_4-NPs prepared using NaOH (without honey) as the reducing agent is 28.98 emu g^{-1} for sample (a). The presence of organic coating agents on sample (b), (c), (d) and (e) decreased the saturation magnetization value compared with sample (a), which decreases the homogeneity caused by the reducing of the surface moments.[50] It is widely identified that the size of magnetic particles has an effect on the energy of that particle in an exterior field through the quantity of magnetic molecules in a single magnetic domain. When the energy is converted into the thermal energy, thermal variations

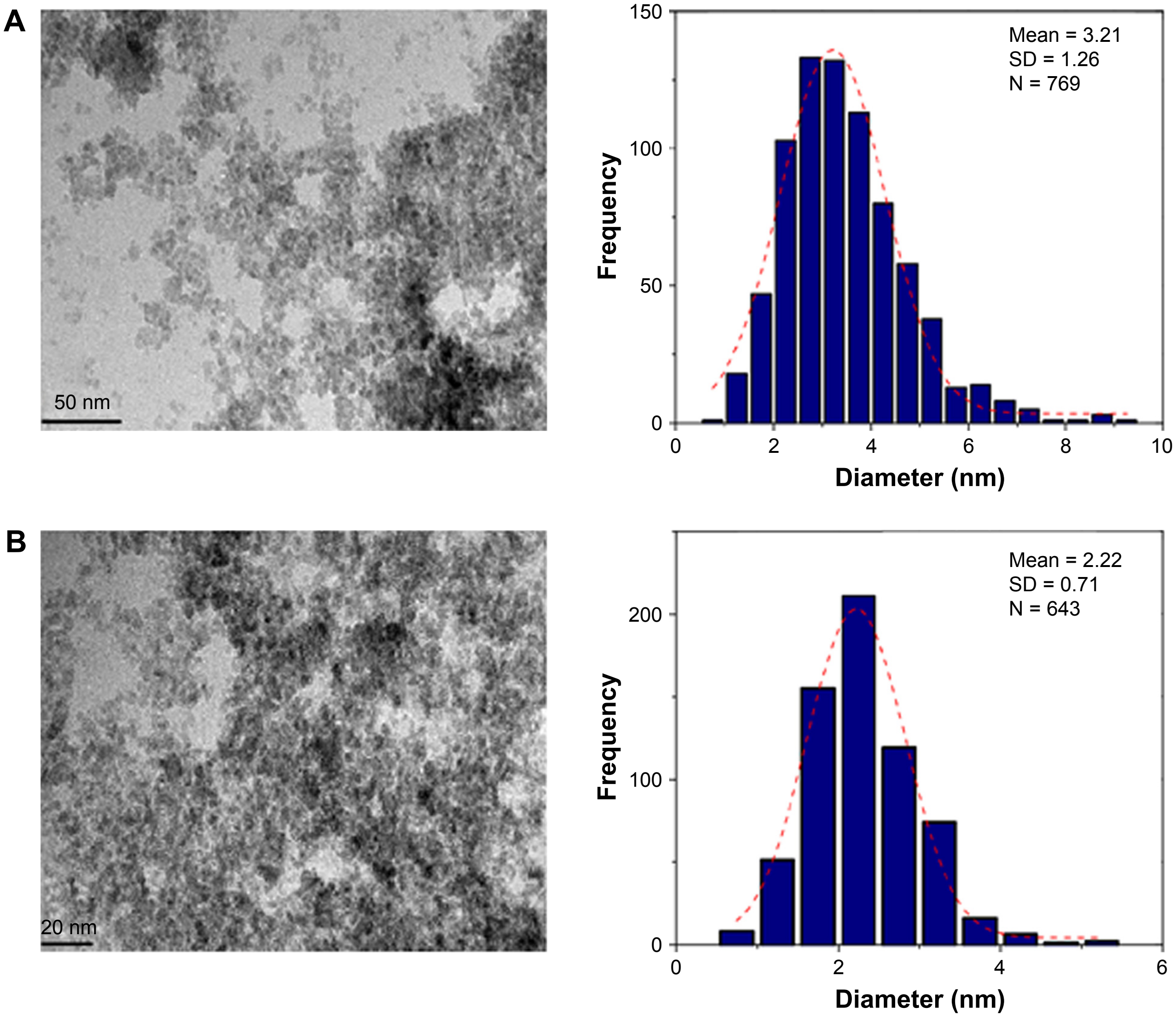

Figure 4 TEM images and histograms of particle size distribution for 0.5% and 3% (w/v) honey/Fe_3O_4-NPs. (**A**) and (**B**): 0.5% and 3% (w/v), respectively.
Abbreviations: Fe_3O_4-NPs, magnetite nanoparticles; TEM, transmission electron microscopy.

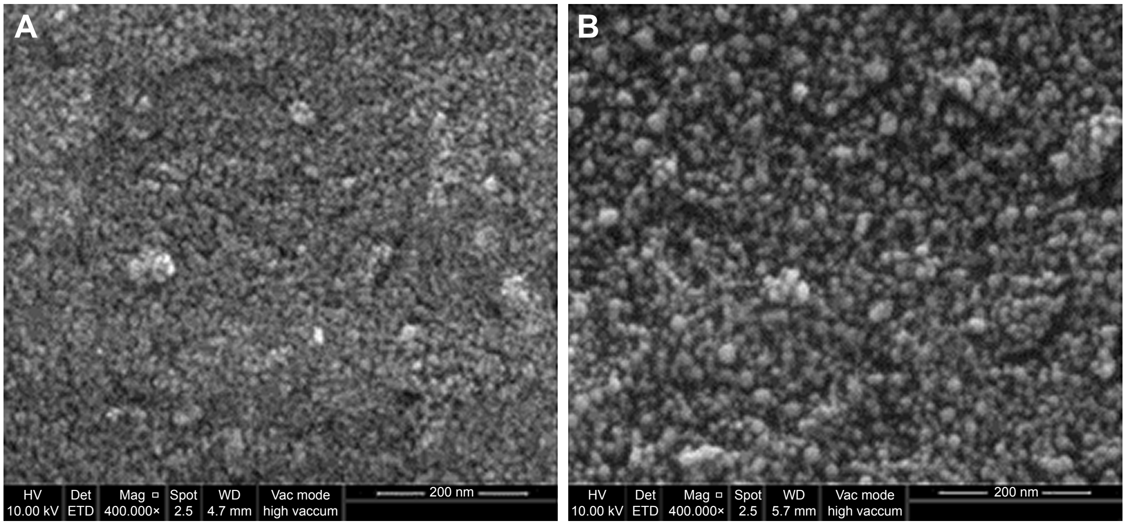

Figure 5 Surface morphology of magnetite nanoparticles with 0.5% and 3% (w/v) honey (**A**) and (**B**), respectively.

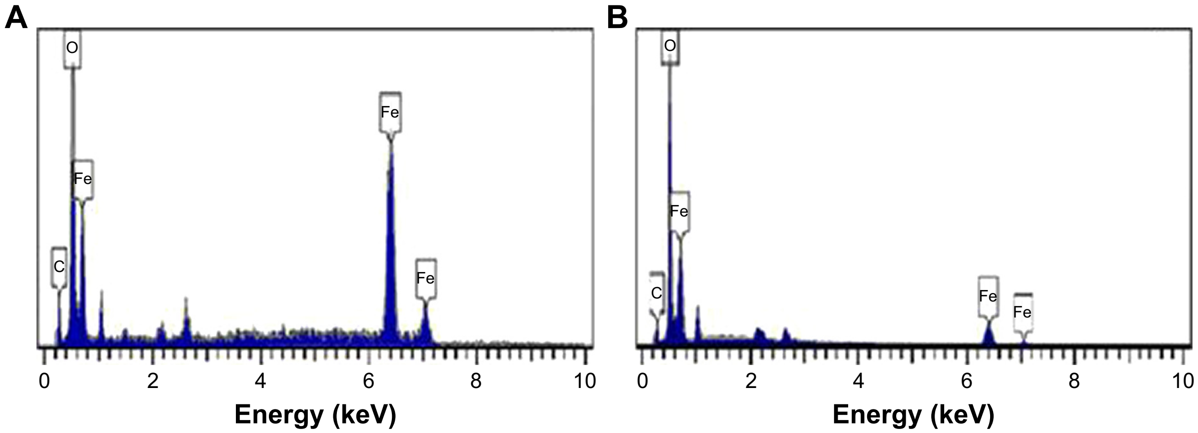

Figure 6 EDX spectroscopy of Fe_3O_4-NPs with 0.5% and 3% (w/v) honey, (**A**) and (**B**), respectively.
Abbreviations: EDX, energy-dispersive X-ray; Fe_3O_4-NPs, magnetite nanoparticles.

around the prepared Fe_3O_4-NPs magnetically disturbed surface, which will considerably decrease the overall magnetic moments of a given field.[51,52] Thus, this circumstance is more critical for smaller nanoparticles because of the more available surface area; consequently the decrease in the saturation magnetization is reasonable. Table 1 gives a comparison between the synthetic methods, particle sizes and saturation magnetization of Fe_3O_4 NPs from the results of other researchers and this work.

Cytotoxicity assay

In vitro cytotoxicity evaluation of Fe_3O_4-NPs was performed by using 3-(4, 5-dimethylthiazol-2-yl)–2,5-diphenyltetrazolium bromide (MTT) assay. The results are shown in Figure 8. Briefly, WEHI164 fibro sarcoma cells (Institute Pastor, Iran) at the density of 1×10^4 cells per well were seeded in 96-well plates and incubated (37°C in 5% CO_2) for 24 hours. Then, various concentrations of Fe_3O_4-NPs were added and incubated for 24 hours. After 24 hours, 20 µL of 5 mg/mL MTT was added and cells were incubated for another 4 hours. Then the medium was removed and 100 µL of DMSO added in each well to dissolve formazan crystals that produced by living cells. In the following, optical absorbance was measured at 570 (630 used as a reference wavelength) by plate reader (Epoch, BioTech instrument, USA). All experiments were performed in quadruplicate,

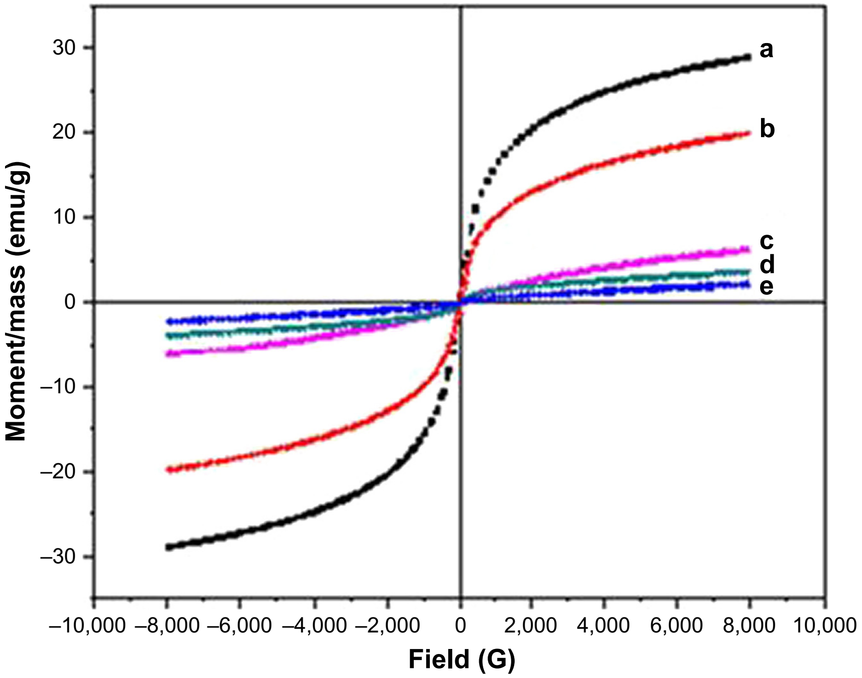

Figure 7 VSM of pure Fe_3O_4 (**a**) and Fe_3O_4-NPs with 0.5, 1, 3 and 5% (w/v) honey (**b–e**, respectively).
Abbreviations: Fe_3O_4-NPs, magnetite nanoparticles; VSM, vibrating sample magnetometry.

Table 1 Comparison between the synthetic methods, particle sizes and saturation magnetization of Fe_3O_4 NPs from the results of other researchers and this work

Method of synthesis	**Particle size (nm)**	**Saturation magnetization (M_s)**	**Reference**
Coprecipitation method using NH_4OH and chitosan	23 nm	15 emu·g^{-1}	53
Quick precipitation using sodium hydroxide and rice straw	9.93 nm	NA	54
Coprecipitation method using NaOH and montmorillonite	8.24–12.88 nm	12.10–32.40 emu·g^{-1}	55
Hydrothermal reduction route using sucrose	4–16 nm	14.82–29.55 emu·g^{-1}	56
Coprecipitation method using NaOH and talc	2.27–8.13 nm	NA	57
Facile technique using diethyl amine	~25 nm	35.76 emu·g^{-1}	58
Coprecipitation method using NaOH and carob leaf extract	4–8 nm	NA	59
Coprecipitation method using aqueous extract of brown seaweed (*Sargassum muticum*)	18 nm	22.1 emu·g^{-1}	60
Coprecipitation method using olive oil (magnetite (Fe_3O_4) and maghemite (γ-Fe_2O_3) nanoparticles)	20 nm	40 emu·g^{-1}	61
Solvothermal synthesis	~200 nm	78.03 emu·g^{-1}	21
Coprecipitation method	10 nm	46.7 emu·g^{-1}	16
Colloidal method at room temperature	4–43 nm	NA	13
Precipitation with forced mixing	~6.0 nm	37.50 emu·g^{-1}	9
Coprecipitation method using NaOH and honey	3.21 nm	19.91 emu·g^{-1}	Current study

Abbreviations: Fe_3O_4-NPs, magnetite nanoparticles; NA, not available.

and % cell viability was shown as a percent relative of untreated control cells.[62–64]

As illustrated in Figure 8, the toxicity of the synthesized Fe_3O_4 Au-NPs to the cells was found to be nonsignificant in higher concentrations up to 140.0 ppm and they were well tolerated by WEHI164 cells in the MTT assay.

Conclusion

This study reports the facile and green synthesis of superparamagnetic Fe_3O_4-NPs using natural honey as the reducing and stabilizing agent. A sharp band at 564 cm^{-1} in the FT-IR spectra supplementary confirmed the presence of Fe_3O_4-NPs. The particle size of the synthesized material can be certainly controlled with the change in the concentration of the natural honey. The TEM images showed that the particle size decreased from 3.21 to 2.22 nm with the increase in the amount of honey from 0.5% to 3.0% (w/v), respectively. The VSM analysis shown a super-paramagnetic behavior of the Fe_3O_4-NPs, with a small magnetization of 19.91 emu·g^{-1} as compared to the Fe_3O_4-NPs prepared in the absence of honey (28.98 emu·g^{-1}), which is related to the nanoparticle size. From the results of these studies, we believe that the present method can be used for the controlled synthesis of Fe_3O_4-NPs, which can find important applications in biotechnology, biosensor and biomedicine, magnetic resonance imaging and catalysis. The most possible co-reducing

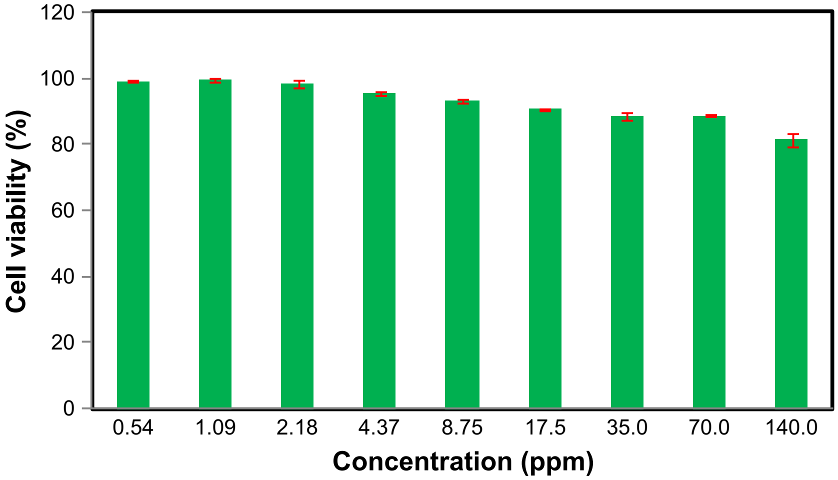

Figure 8 Cell viability of WEHI164 cells measured by the MTT assay (cells were incubated for 24 hours with the indicated concentrations of the magnetite nanoparticles).

agent is fructose and the existence proteins in the natural honey as the capping agent is responsible for stabilization.

Acknowledgments

We would like to acknowledge the financial support provided by University of Malaya under the Equitable Society Research Cluster (ESRC) research grant GC001C-14SBS.

Disclosure

The authors report no conflicts of interest in this work.

References

1. Khandanlou R, Ahmad MB, Fard Masoumi HR, Shameli K, Basri M, Kalantari K. Rapid adsorption of copper(II) and lead(II) by rice straw/Fe_3O_4 nanocomposite: optimization, equilibrium isotherms, and adsorption kinetics study. *PLoS One*. 2015;10(3):e0120264.
2. Bogunia-Kubik K, Sugisaka M. From molecular biology to nanotechnology and nanomedicine. *Biosystems*. 2002;65(2–3):123–138.
3. Daniel MC, Astruc D. Gold nanoparticles: assembly, supramolecular chemistry, quantum-size-related properties, and applications toward biology, catalysis, and nanotechnology. *Chem Rev*. 2004;104(1):293–346.
4. Zharov VP. Self-assembling nanoclusters in living systems: application for integrated photothermal nanodiagnostics and nanotherapy. *Nanomedicine*. 2005;1(4):326–345.
5. Qiao R, Yang C, Gao M. Superparamagnetic iron oxide nanoparticles: from preparations to in vivo MRI applications. *J Mater Chem*. 2009;19(35):6274–6293.
6. Silva CR, Fonseca MG, Barone JS, Airoldi C. Layered Inorganic–Organic Talc-like Nanocomposites. *Chem Mater*. 2002;14(1):175–179.
7. Park J, An K, Hwang Y, et al. Ultra-large-scale syntheses of monodisperse nanocrystals. *Nat Mater*. 2004;3(12):891–895.
8. Yu W, Zhang T, Zhang J, Qiao X, Yang L, Liu Y. The synthesis of octahedral nanoparticles of magnetite. *Mater Lett*. 2006;60(24):2998–3001.
9. Zhu Y, Wu Q. Synthesis of magnetite nanoparticles by precipitation with forced mixing. *J Nanopart Res*. 1999;1(3):393–396.
10. Maity D, Chandrasekharan P, Yang CT, et al. Facile synthesis of water-stable magnetite nanoparticles for clinical MRI and magnetic hyperthermia applications. *Nanomedicine*. 2010;5(10):1571–1584.
11. Cai W, Wan J. Facile synthesis of superparamagnetic magnetite nanoparticles in liquid polyols. *J Colloid Interface Sci*. 2007;305(2):366–370.
12. Vijayaákumar R. Preparation of amorphous magnetite nanoparticles embedded in polyvinyl alcohol using ultrasound radiation. *J Mater Chem*. 2000;10(5):1125–1129.
13. Martínez-Mera I, Espinosa-Pesqueira ME, Pérez-Hernández R, Arenas-Alatorre J. Synthesis of magnetite (Fe3O4) nanoparticles without surfactants at room temperature. *Mater Lett*. 2007;61(23–24):4447–4451.
14. Pinna N, Grancharov S, Beato P, Bonville P, Antonietti M, Niederberger M. Magnetite Nanocrystals: Nonaqueous Synthesis, Characterization, and Solubility. *Chem Mater*. 2005;17(11):3044–3049.
15. Chiu WS, Radiman S, Abdullah MH, Khiew PS, Huang NM, Abd-Shukor R. One pot synthesis of monodisperse Fe3O4 nanocrystals by pyrolysis reaction of organometallic compound. *Mater Chem Phys*. 2007;106(2–3):231–235.
16. El Ghandoor H. Synthesis and some physical properties of magnetite (Fe3O4) nanoparticles. *Int J Electrochem Sci*. 2012;7(6):5734–5745.
17. Maity D, Kale SN, Kaul-Ghanekar R, Xue J-M, Ding J. Studies of magnetite nanoparticles synthesized by thermal decomposition of iron (III) acetylacetonate in tri(ethylene glycol). *J Magn Magn Mater*. 2009;321(19):3093–3098.
18. Woo K, Hong J, Choi S, et al. Easy synthesis and magnetic properties of iron oxide nanoparticles. *Chem Mater*. 2004;16(14):2814–2818.
19. Pei W, Kumada H, Natusme T, Saito H, Ishio S. Study on magnetite nanoparticles synthesized by chemical method. *J Magn Magn Mater*. 2007;310(2):2375–2377.
20. Mizutani N, Iwasaki T, Watano S, Yanagida T, Tanaka H, Kawai T. Effect of ferrous/ferric ions molar ratio on reaction mechanism for hydrothermal synthesis of magnetite nanoparticles. *Bull Mater Sci*. 2008;31(5):713–717.
21. Zhang W, Shen F, Hong R. Solvothermal synthesis of magnetic Fe3O4 microparticles via self-assembly of Fe3O4 nanoparticles. *Particuology*. 2011;9(2):179–186.
22. Han C, Cai W, Tang W, Wang G, Liang C. Protein assisted hydrothermal synthesis of ultrafine magnetite nanoparticle built-porous oriented fibers and their structurally enhanced adsorption to toxic chemicals in solution. *J Mater Chem*. 2011;21(30):11188–11196.
23. Bretcanu O, Verné E, Cöisson M, Tiberto P, Allia P. Magnetic properties of the ferrimagnetic glass-ceramics for hyperthermia. *J Magn Magn Mater*. 2006;305(2):529–533.
24. Jun YW, Huh YM, Choi JS, et al. Nanoscale size effect of magnetic nanocrystals and their utilization for cancer diagnosis via magnetic resonance imaging. *J Am Chem Soc*. 2005;127(16):5732–5733.
25. Osaka T, Matsunaga T, Nakanishi T, Arakaki A, Niwa D, Iida H. Synthesis of magnetic nanoparticles and their application to bioassays. *Anal Bioanal Chem*. 2006;384(3):593–600.
26. Peng S, Wang C, Xie J, Sun S. Synthesis and stabilization of monodisperse Fe nanoparticles. *J Am Chem Soc*. 2006;128(33):10676–10677.
27. Sun S, Zeng H, Robinson DB, et al. Monodisperse MFe2O4 (M = Fe, Co, Mn) nanoparticles. *J Am Chem Soc*. 2004;126(1):273–279.
28. Ayala-Valenzuela O, Matutes-Aquino J, Betancourt-Galindo R, et al. Magnetite-cobalt ferrite nanoparticles for kerosene-based magnetic fluids. *J Magn Magn Mater*. 2005;294(2):e37–e41.
29. Kalantari K, Bin Ahmad M, Shameli K, Khandanlou R. Synthesis of talc/Fe_3O_4 magnetic nanocomposites using chemical co-precipitation method. *Int J Nanomedicine*. 2013;8:1817–1823.
30. White JW Jr. Honey. In: *Advances in Food Research*. Volume 24. Cambridge, MA: Academic Press; 1978:287–374.
31. Singh N, Bath PK. Quality evaluation of different types of Indian honey. *Food Chem*. 1997;58(1–2):129–133.
32. Terrab A, Díez MJ, Heredia FJ. Characterisation of Moroccan unifloral honeys by their physicochemical characteristics. *Food Chem*. 2002;79(3):373–379.
33. Nanda V, Sarkar BC, Sharma HK, Bawa AS. Physico-chemical properties and estimation of mineral content in honey produced from different plants in Northern India. *J Food Compost Anal*. 2003;16(5):613–619.
34. Devillers J, Morlot M, Pham-Delègue MH, Doré JC. Classification of monofloral honeys based on their quality control data. *Food Chem*. 2004;86(2):305–312.
35. Karaoğlu E, Baykal A, Erdemi H, Alpsoy L, Sozeri H. Synthesis and characterization of dl-thioctic acid (DLTA)–Fe3O4 nanocomposite. *J Alloys Compd*. 2011;509(37):9218–9225.
36. Chen X, Yu J, Zhang Z, Lu C. Study on structure and thermal stability properties of cellulose fibers from rice straw. *Carbohydr Polym*. 2011;85(1):245–250.
37. Li S, Shen Y, Xie A, et al. Rapid, room-temperature synthesis of amorphous selenium/protein composites using Capsicum annuum L extract. *Nanotechnology*. 2007;18(40):405101.
38. Philip D. Biosynthesis of Au, Ag and Au-Ag nanoparticles using edible mushroom extract. *Spectrochim Acta A Mol Biomol Spectrosc*. 2009;73(2):374–381.
39. Philip D. Honey mediated green synthesis of gold nanoparticles. *Spectrochim Acta A Mol Biomol Spectrosc*. 2009;73(4):650–653.

40. Basavaraja S, Balaji SD, Lagashetty A, Rajasab AH, Venkataraman A. Extracellular biosynthesis of silver nanoparticles using the fungus Fusarium semitectum. *Mater Res Bull*. 2008;43(5):1164–1170.
41. Ahmad A, Senapati S, Khan MI, Kumar R, Sastry M. Extracellular biosynthesis of monodisperse gold nanoparticles by a novel extremophilic actinomycete, *Thermomonospora* sp. *Langmuir*. 2003;19(8):3550–3553.
42. Shankar SS, Ahmad A, Pasricha R, Khan MI, Kumar R, Sastry M. Immobilization of biogenic gold nanoparticles in thermally evaporated fatty acid and amine thin films. *J Colloid Interface Sci*. 2004;274(1):69–75.
43. Solomun T, Schimanski A, Sturm H, Illenberger E. Reactions of amide group with fluorine as revealed with surface analytics. *Chem Phys Lett*. 2004;387(4–6):312–316.
44. Huang J, Li Q, Sun D, et al. Biosynthesis of silver and gold nanoparticles by novel sundried *Cinnamomum camphora* leaf. *Nanotechnology*. 2007;18(10):105104.
45. Ankamwar B, Chaudhary M, Sastry M. Gold nanotriangles biologically synthesized using tamarind leaf extract and potential application in vapor sensing. *Synth React Inorg Met Org Nano Metal Chem*. 2005;35(1):19–26.
46. Cushing BL, Kolesnichenko VL, O'Connor CJ. Recent advances in the liquid-phase syntheses of inorganic nanoparticles. *Chem Rev*. 2004;104(9):3893–3946.
47. Chen J, Wang F, Huang K, Liu Y, Liu S. Preparation of Fe3O4 nanoparticles with adjustable morphology. *J Alloys Compd*. 2009;475(1–2):898–902.
48. Li Z, Sun Q, Gao M. Preparation of water-soluble magnetite nanocrystals from hydrated ferric salts in 2-pyrrolidone: mechanism leading to Fe_3O_4. *Angew Chem Int Ed Engl*. 2005;44(1):123–126.
49. Goya GF, Berquó TS, Fonseca FC, Morales MP. Static and dynamic magnetic properties of spherical magnetite nanoparticles. *J Appl Phys*. 2003;94(5):3520–3528.
50. Kim DK, Mikhaylova M, Zhang Y, et al. Protective coating of superparamagnetic iron oxide nanoparticles. *Chem Mater*. 2003;15(8):1617–1627.
51. Chantrell R, Popplewell J, Charles S. Measurements of particle size distribution parameters in ferrofluids. *IEEE Trans Magn*. 1978;14(5):975–977.
52. Shafi KVPM, Gedanken A, Prozorov R, Balogh J. Sonochemical Preparation and Size-Dependent Properties of Nanostructured $CoFe_2O_4$ Particles. *Chem Mater*. 1998;10(11):3445–3450.
53. Dung DTK, Hai TH, Phuc LH, Long BD, Vinh LK, Truc PN. Preparation and characterization of magnetic nanoparticles with chitosan coating. *J Phys: Conf Ser*. 2009;187(1):012036.
54. Khandanlou R, Bin Ahmad M, Shameli K, Kalantari K. Synthesis and characterization of rice straw/Fe3O4 nanocomposites by a quick precipitation method. *Molecules*. 2013;18(6):6597–6607.
55. Kalantari K, Ahmad MB, Shameli K, Hussein MZB, Khandanlou R, Khanehzaei H. Size-Controlled synthesis of Fe_3O_4 magnetic nanoparticles in the layers of montmorillonite. *J Nanomater*. 2014:739485.
56. Sun X, Zheng C, Zhang F, et al. Size-Controlled Synthesis of Magnetite (Fe_3O_4) Nanoparticles Coated with Glucose and Gluconic Acid from a Single Fe(III) Precursor by a Sucrose Bifunctional Hydrothermal Method. *J Phys Chem C*. 2009;113(36):16002–16008.
57. Kalantari K, Ahmad MB, Shameli K, et al. Size-controlled synthesis of Fe3O4 magnetite nanoparticles on the exterior of talc layers. *Res Chem Intermed*. 2015;41(4):2139–2151.
58. Ahmad S, Riaz U, Kaushik A, Alam J. Soft template synthesis of super paramagnetic Fe_3O_4 nanoparticles a novel technique. *J Inorg Organomet Polym Mater*. 2009;19(3):355–360.
59. Awwad AM, Salem NM. A Green and Facile Approach for Synthesis of Magnetite Nanoparticles. *Nanosci Nanotechnol*. 2012;2(6):208–213.
60. Mahdavi M, Namvar F, Ahmad MB, Mohamad R. Green biosynthesis and characterization of magnetic iron oxide (Fe_3O_4) nanoparticles using seaweed (Sargassum muticum) aqueous extract. *Molecules*. 2013;18(5):5954–5964.
61. Palanisamy K. Synthesis and characterization of olive oil mediated iron oxide nanoparticles. *Dig J Nanomater Biostruct*. 2013;8(2):607–612.
62. Mokhodoeva O, Vlk M, Málková E, et al. Study of 223Ra uptake mechanism by Fe_3O_4 nanoparticles: towards new prospective theranostic SPIONs. *J Nanopart Res*. 2016;18(10):301.
63. Lahooti A, Sarkar S, Saligheh Rad H, et al. PEGylated superparamagnetic iron oxide nanoparticles labeled with 68Ga as a PET/MRI contrast agent: a biodistribution study. *J Radioanal Nucl Chem*. 2017;311(1):769–774.
64. Sharkey J, Starkey Lewis PJ, Barrow M, et al. Functionalized superparamagnetic iron oxide nanoparticles provide highly efficient iron-labeling in macrophages for magnetic resonance-based detection in vivo. *Cytotherapy*. 2017;19(4):555–569.